IEEE Access
Multidisciplinary | Rapid Review | Open Access Journal

Received March 2, 2020, accepted March 21, 2020, date of publication March 27, 2020, date of current version April 13, 2020.

Digital Object Identifier 10.1109/ACCESS.2020.2983823

A Soft Computing Approach Based on Fractional Order DPSO Algorithm Designed to Solve the Corneal Model for Eye Surgery

W. WASEEM[1], MUHAMMAD SULAIMAN[1], AHMAD ALHINDI[2,3], (Member, IEEE), AND HOSAM ALHAKAMI[2]

[1]Department of Mathematics, Abdul Wali Khan University Mardan, Mardan 23200, Pakistan
[2]Department of Computer Science, Umm Al-Qura University, Makkah 21955, Saudi Arabia
[3]Center of Innovation and Development in AI (CIADA), Umm Al-Qura University, Makkah 21955, Saudi Arabia

Corresponding authors: Muhammad Sulaiman (msulaiman@awkum.edu.pk) and Ahmad Alhindi (ahhindi@uqu.edu.sa)

This work was supported by the Umm Al-Qura University, Makkah, Saudi Arabia.

ABSTRACT In this research, a soft computing approach based on a Nature-inspired technique, the Fractional-Order Darwinian Particle Swarm Optimization (FO-DPSO) algorithm, is hybridized with feed-forward artificial neural network (FF-ANN) to suggest and calculate better solutions for non-linear second-order ordinary differential equation (ODE) representing the corneal shape model (CSM). The unknown weights involved in approximate solutions obtained through ANN are tuned with the help of FO-DPSO. To test the robustness of our approach and conditionality of CSM, we have considered several cases of CSM with different aspects of the problem. Solutions obtained by Adam's method are used as a reference point for the sake of comparison. We establish it that FO-DPSO is a suitable technique for tuning the unknown weights involved in the solution designed with ANNs. Our results suggest that the proposed approach is a suitable candidate for solving real-world problems involving differential equations.

INDEX TERMS Non-linear differential equations, meta-heuristics, soft computing, corneal shape model, feed-forward artificial neural networks, fractional order Darwinian particle swarm optimization.

I. INTRODUCTION

The transparent front part of the eye known as corneal is represented by its curvature model. Its mathematical model is called corneal shape model (CSM), and mathematically it is given in [1] as

$$\begin{cases} \left(\dfrac{\chi'}{\sqrt{1+\chi'^2}}\right)' - c\chi + \dfrac{d}{\sqrt{1+\chi'^2}} = 0 \text{ in } [0,1], \\ \chi'(0) = \chi(1) = 0. \end{cases} \tag{1}$$

where c, d are non-zero constant values. A generalized n-dimensional form of CSM is given as

$$\begin{cases} \text{div}\left(\dfrac{\nabla\chi}{\sqrt{1+|\nabla\chi|^2}}\right) = c\chi - \dfrac{d}{\sqrt{1+|\nabla\chi|^2}}, & \text{in } \Omega. \\ \chi & \text{on } \partial\Omega. \end{cases} \tag{2}$$

The associate editor coordinating the review of this manuscript and approving it for publication was Nizam Uddin Ahamed.

Equation (2) is a mathematical description of the shape of the human corneal [2]–[4]. The bounded domain in $\Omega \in R^n$ represents a Lipschitz domain and $div\left(\dfrac{\nabla\chi}{\sqrt{1+|\nabla\chi|^2}}\right)$ is a mean curvature. As a special case, using values of $d \in]0, \frac{3\sqrt{3}}{2}\frac{\sqrt{c}}{tanh\sqrt{c}}[$ CSM in (1) is given as,

$$\begin{cases} \chi'' - c\chi + \dfrac{d}{\sqrt{1+\chi'^2}} = 0, \\ \chi'(0) = \chi(1) = 0 \quad \text{in } [0,1]. \end{cases} \tag{3}$$

The special curvature of corneal deflects higher intensity of lights and protects internal part of the human eye [2]. The eye cornea is further classified into five types of layers,

(a) Innermost endothelium.
(b) Descemet's membrane.
(c) Outermost epithelium.
(d) The Stroma.
(e) The Bowman's layer.

Stroma is formed of cells known as quiescent stromal cells and well-organized collagen fibrils. Stroma forms 90%

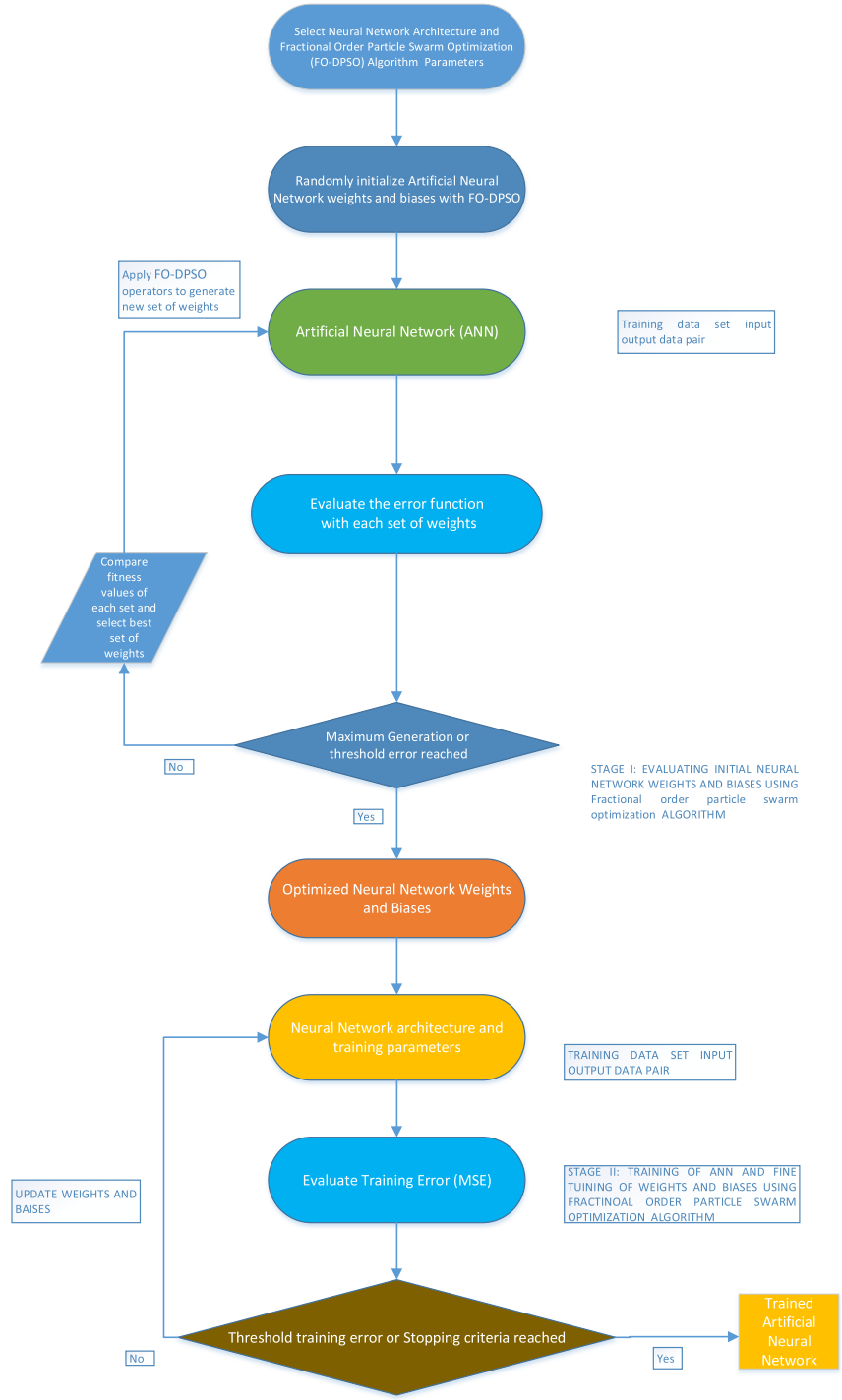

FIGURE 1. **Graphical abstract of our soft computing design.**

of thickness for cornea [4], [5]. With the help of stroma, eyesight is transparent. The collagen diameter, proteoglycans, orthogonal lamellae and spacing of fibrils play a vital role in the health of stroma [6]–[9]. Many techniques are used to handle highly non-linear boundary value problems (BVPs), we have reviewed a list of such techniques, like, differential transform method [10] Adomian decomposition method [11], variational iterative technique [12] and Spline interpolation [13]. Problems are also solved by methods involving Green's functions. For instance, Malekzadeh *et al.* [14] revisited the model of freely vibrating, elastic, functionally graded circular plates with varying thickness. He used Green's and Quasi Green's functions to study his models. Andrade [15] suggested an approach based on the exact Green's function

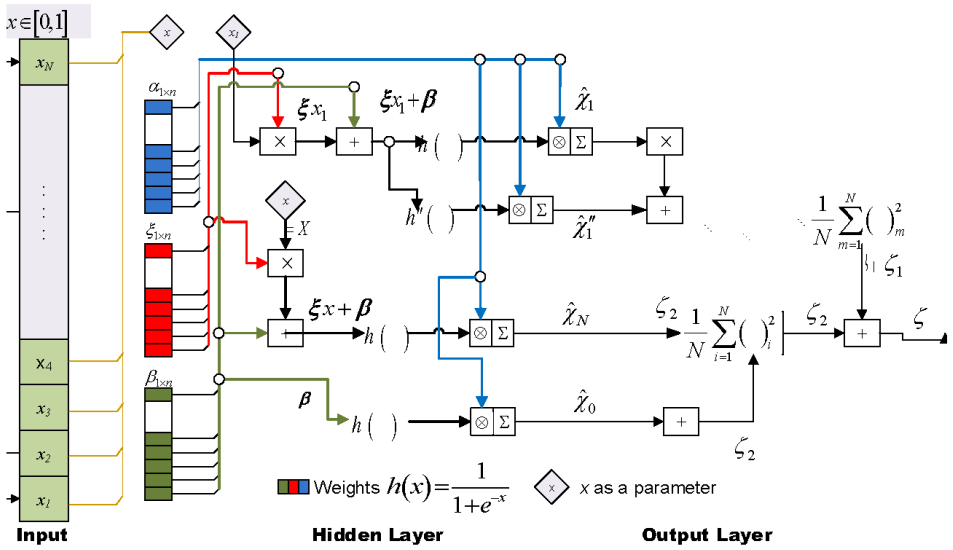

FIGURE 2. Architecture of the neural network for approximate solution of CSM [41].

for the arbitrary rectangular potentials. Ahyoune *et al.* [16] employed a multi-objective Green's function of 2D and 3D having different weights to solve quasi-static partial element equivalent circuits. Problems arising in the fields of oscillation theory, ignition, and electro-analytical chemistry are solved with the help of a coupled Green's function together with an iterative technique. These problems include Bratu differential equations [17]–[19]. All these procedures have their effectiveness, exactness, robustness, and other characteristics like the ease of implementation, requirement of prior knowledge about the problem and weaknesses over one another. In [20]–[22], they combine ANNs with random search techniques to tackle biological models represented through differential equations. These artificial intelligence schemes are suitable to calculate solutions for the CSM. Many researchers had worked on the said scheme which includes solvers are in electromagnetic [23], circuit theory [24], fuel ignition model [25], Thomas-Fermi model [26], induction of the motor models [27], doubly singular nonlinear systems [27], nanofluidics [28], nanotechnology [29], nonlinear prey-predator models [30], Troesch's problem [31], nonlinear equations [32], optimal control [33], mathematical modeling and control theory of particle accelerators [34], signal processing [35], linear and nonlinear fractional order model [36], financial mathematics [37], physical models signified nonlinear system of equations [38] and powerfully nonlinear differential equations with many singularities of Painleve equations [39]. Recently, the design analysis of porous fins is studied with the help of a combined procedure CS-ANN in [40]. In [41], a hybrid approach of Particle Swarm Optimization (PSO) together with the Active set algorithm (ASA), namely PSO-ASA, is used to solve CSM. Keeping this in view, it motivates the authors to design a simple to implement a single optimization technique that will use fewer iterations and memory to achieve the best solutions for CSM. To minimize the mean squared error in the solutions formed by ANNs, we use an efficient single meta-heuristic technique named as FO-DPSO to achieve this task. The following features of the suggested method is briefly given as:

- We will use ANNs to design approximate solutions for CSM. We will train the unknown weights involved in the solutions to produce consistent solutions.
- The proposed methodology is efficiently applied for different cases of the CSM, which shows better performance of the scheme.
- We had compared the results of the proposed scheme FO-DPSO with PSO-ASA numerical technique available in the literature.
- The statistical analysis has been done for the proposed scheme and compared the results with other optimization techniques based on mean squared error, mean absolute error, mean absolute deviation and standard deviation.
- Along with calculating consistent instantaneous solutions, we will concentrate on ease of implementation, smoothness of algorithm, simplicity, reliability of our soft computing design for CSM.
- Our approach is based on a single optimization technique which is effective in term of computational cost like execution time, function evaluation and number of iteration as compared to PSO-ASA which is the combination of two algorithms.

We give the organization of the article as the CSM model is described in section 2 which comprises ANNs models and optimization scheme of FO-DPSO. We present performance metrics in section 3. In section 4, we present the numerical results and graphical overview of the CSM. The last section describes the conclusion.

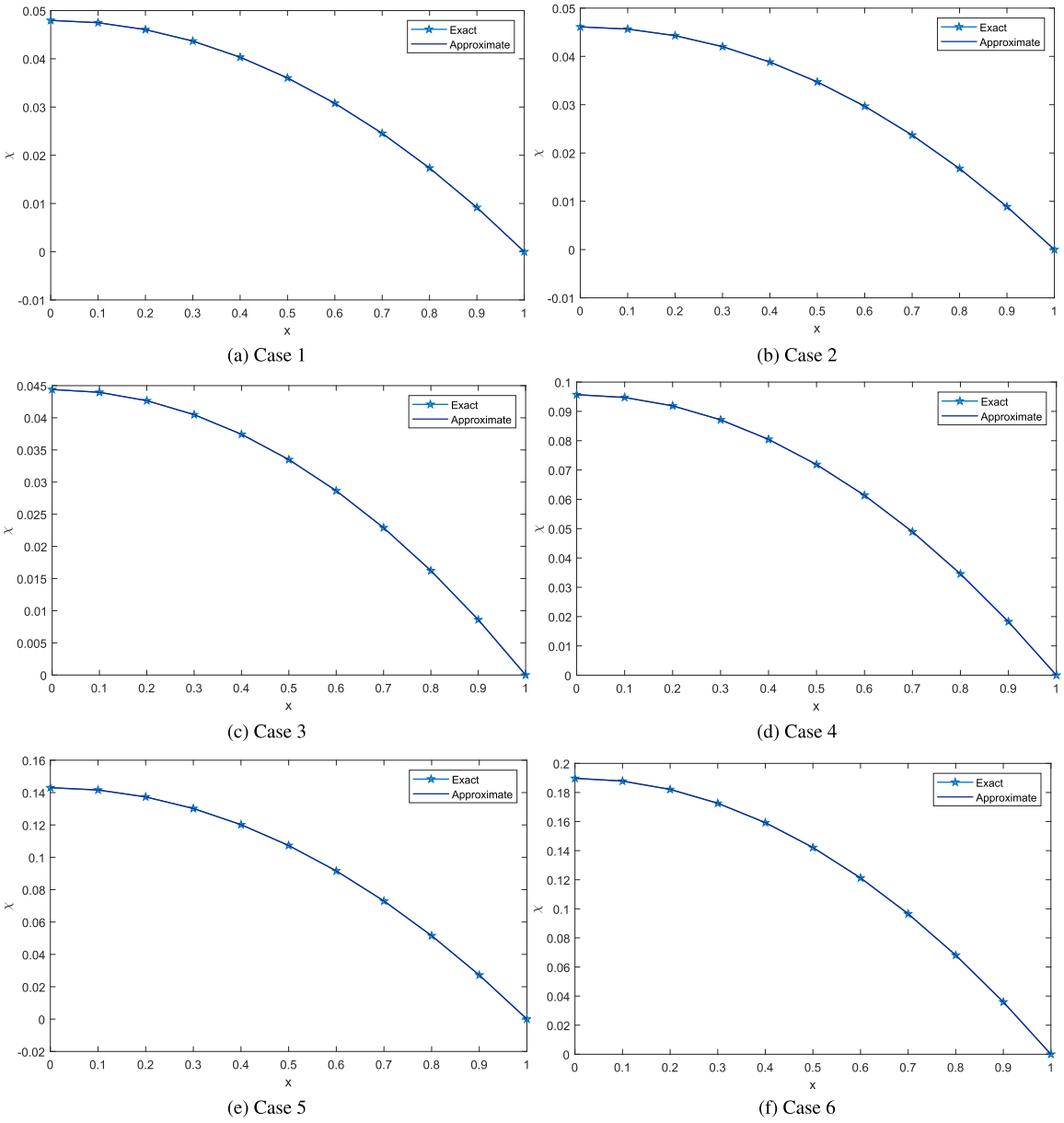

(a) Case 1 (b) Case 2

(c) Case 3 (d) Case 4

(e) Case 5 (f) Case 6

FIGURE 3. Solution plots for six cases.

II. MATHEMATICAL MODEL

It is often hard to solve a non-linear differential equation and is often challenging and difficult to handle. To investigate the solution of such a differential equation, we need an efficient method. In this article, we proposed an ANN-based method. We have divided our findings into two parts. The first part contains a mean-squared error based objective function. While the second part elaborates on the complete process of the training of unknown weights involved in ANN-based solutions and utilization of FDPSO. We give the solution design for the CSM in Fig.1. A flowchart of the whole soft computing scheme involving ANNs and FO-DPSO is presented in Fig.2.

A. MODELING OF APPROXIMATE SOLUTIONS BY UNSUPERVISED NEURAL NETWORKS

Many researchers have found that through artificial neural networks we can find the approximate solution of different mathematical models arising in different fields [42]–[44]. In this research, we designed feed-forward ANNs based solutions for the biological CSM which is represented by a differential equation. Design of continuous maps which suggest the approximate solution $\hat{\chi}(x)$ and its mth order derivative $\hat{\chi}^{(m)}(x)$, are given in equation (4) and (5):

$$\hat{\chi}(x) = \sum_{i=1}^{N} \alpha_i f(\xi_i x + \beta_i) \tag{4}$$

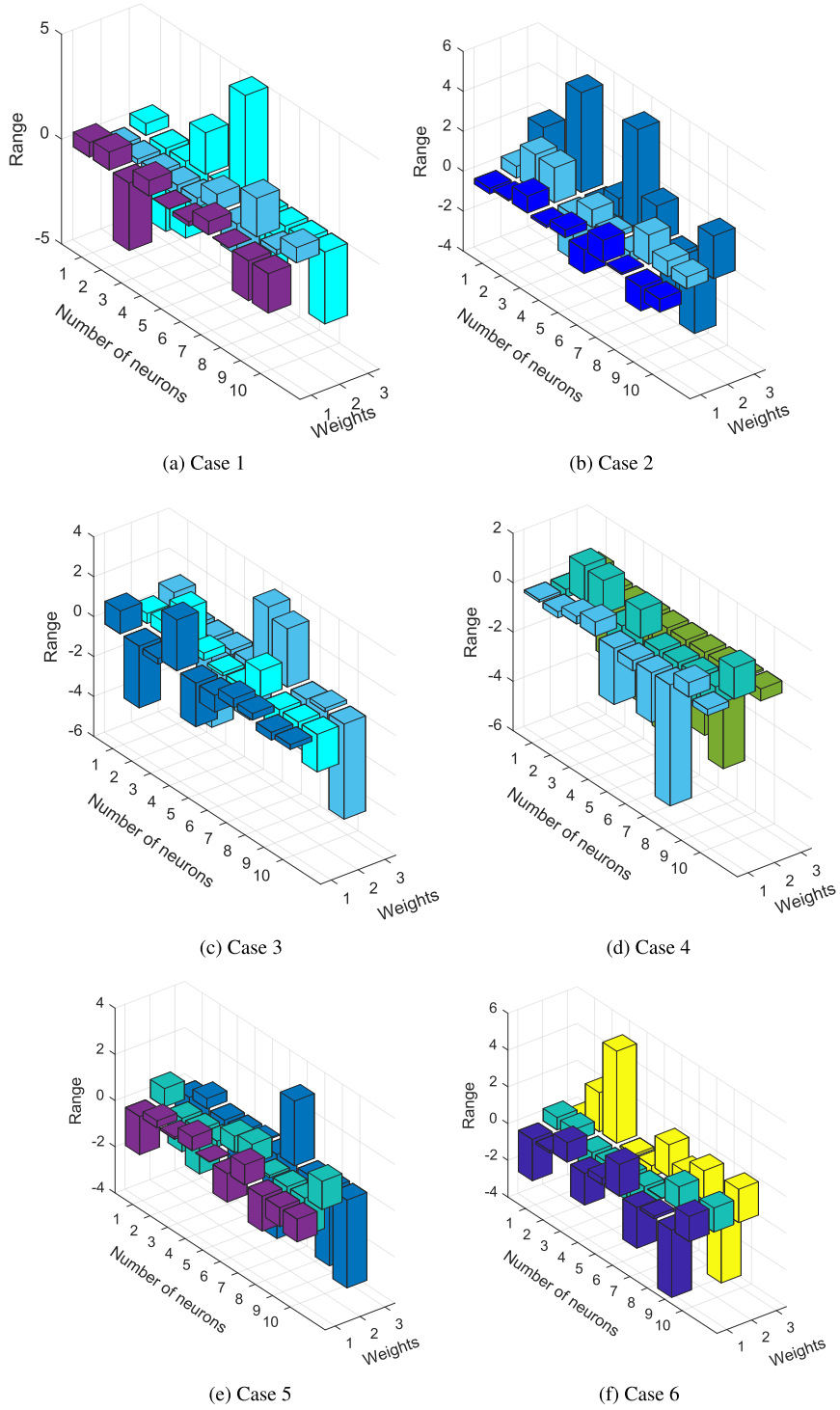

(a) Case 1 (b) Case 2

(c) Case 3 (d) Case 4

(e) Case 5 (f) Case 6

FIGURE 4. Plots of unknown weights for best solutions of six cases.

$$\hat{\chi}^{(m)}(x) = \sum_{i=1}^{N} \alpha_i f^{(m)}(\xi_i x + \beta_i) \tag{5}$$

represents the i^{th} component of α_i, ξ_i and β_i vectors. Moreover, n represents the number of neurons and m denotes the mth derivative of the function. In this research, we consider the log-sigmoid function as an activation function represented mathematically as $f(x) = \frac{1}{1+e^{-x}}$. Using this function equation (4) and (5) becomes:

$$\hat{\chi}(x) = \sum_{j=1}^{n} \alpha_j \left(\frac{1}{1 + e^{-(\xi_j x + \beta_j)}} \right) \tag{6}$$

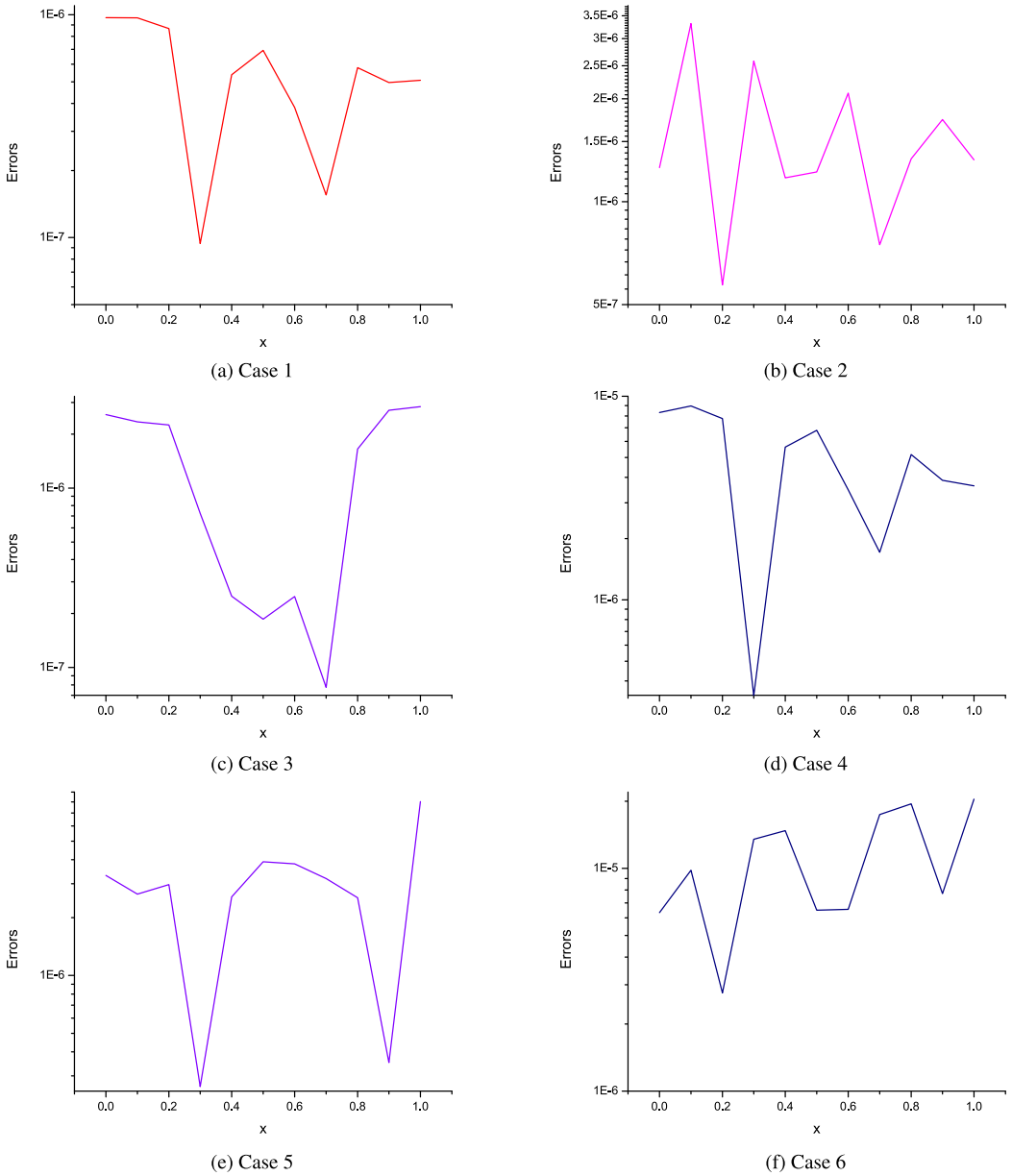

(a) Case 1 (b) Case 2

(c) Case 3 (d) Case 4

(e) Case 5 (f) Case 6

FIGURE 5. Residual errors in best solutions obtained for six cases.

$$\hat{\chi}^{(m)}(x) = \sum_{j=1}^{n} \alpha_j \left(\frac{1}{1 + e^{-(\xi_j x + \beta_j)}} \right)^{(m)} \tag{7}$$

In the case of CSM, the second derivative is used and represented as in equation (8),

$$\hat{\chi}'' = \sum_{j=1}^{n} \alpha_j \xi_j^2 \times \left(\frac{2e^{-2(\xi_j \times t\beta_j)}}{\left(1 + e^{-(\xi_j x + \beta_j)}\right)^3} - \frac{e^{-(\xi_j x + \beta_j)}}{\left(1 + e^{-(\xi_j x + \beta_j)}\right)^2} \right) \tag{8}$$

The combination of the equations given in (6) and equation (8) formulate the objective function for the system represented in equation (3). The error function is given as:

$$\min \zeta = \zeta_1 + \zeta_2, \tag{9}$$

where, ζ_1 is the error function for CSM describes as:

$$\zeta_1 = \frac{1}{N} \sum_{k=1}^{N} (\sqrt{1 + \chi'^2}\hat{\chi}_k'' - c\sqrt{1 + \chi'^2}\hat{\chi} + d)^2$$
$$N = \frac{1}{h}, \quad \hat{\chi}_k = \hat{\chi}(x_k), \quad x_k = kh \tag{10}$$

Similarly, ζ_2 error in the boundary conditions is given in equation (11):

$$\zeta_2 = \frac{1}{2} \left((\hat{\chi}_0')^2 + (\hat{\chi}_N - 1)^2 \right) \tag{11}$$

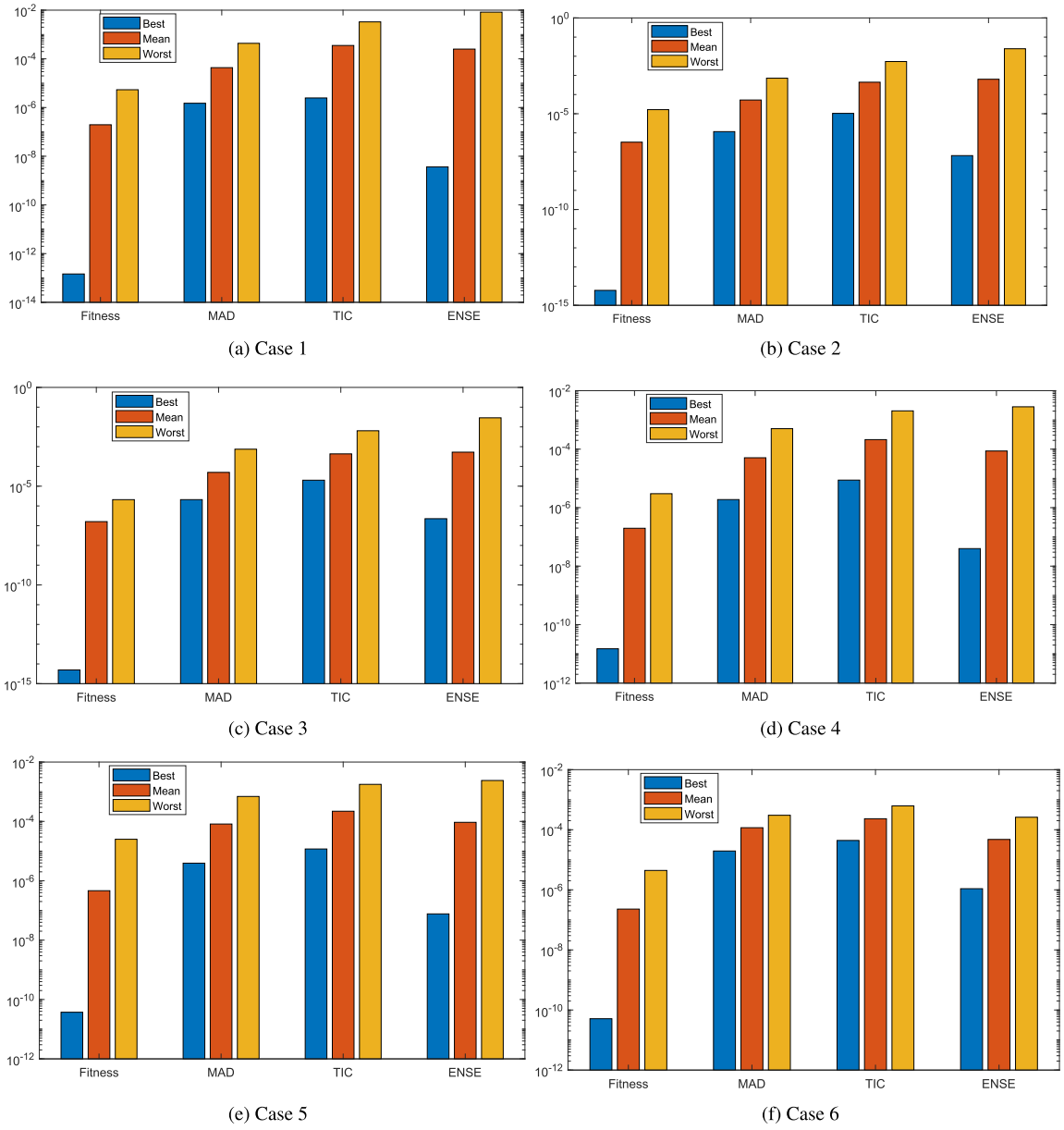

(a) Case 1 (b) Case 2

(c) Case 3 (d) Case 4

(e) Case 5 (f) Case 6

FIGURE 6. Best, mean, and worse values of (a) fitness function (b) MAD (C) TIC (d) ENSE for 100 experiments done for six cases.

B. BASIC DEFINITION FOR FRACTIONAL CALCULUS

Fractional calculus (FC) has attracted the attention of several researchers [46], being applied in various scientific fields such as engineering, computational mathematics, and fluid mechanics, among others. FC can be considered as a generalization of integer-order calculus, thus accomplishing what integer-order calculus cannot. As a natural extension of the integer (i.e., classical) derivatives, fractional derivatives provide an excellent instrument for the description of memory and hereditary properties of processes. The concept of the Grünwald–Letnikov fractional differential is presented by the following definition.

Definition 1: Let Γ be the gamma function defined as [47]

$$\Gamma(k) = (k-1)!. \tag{12}$$

The signal $D^{\alpha}[x(t)]$ given by

$$D^{\alpha}[x(t)] = \lim_{h \to 0} \left[\frac{1}{h^{\alpha}} \sum_{k=0}^{+\infty} \frac{(-1)^k \Gamma(\alpha+1) x(\text{t-k}h)}{\Gamma(k+1)\Gamma(\alpha-k+1)} \right] \tag{13}$$

is said to be the Grünwald–Letnikov fractional derivative of order α, $\alpha \in C$, of a generic signal $x(t)$. An important property revealed by equation (13) is that although an integer-order derivative just implies a finite series, the fractional-order derivative requires an infinite number

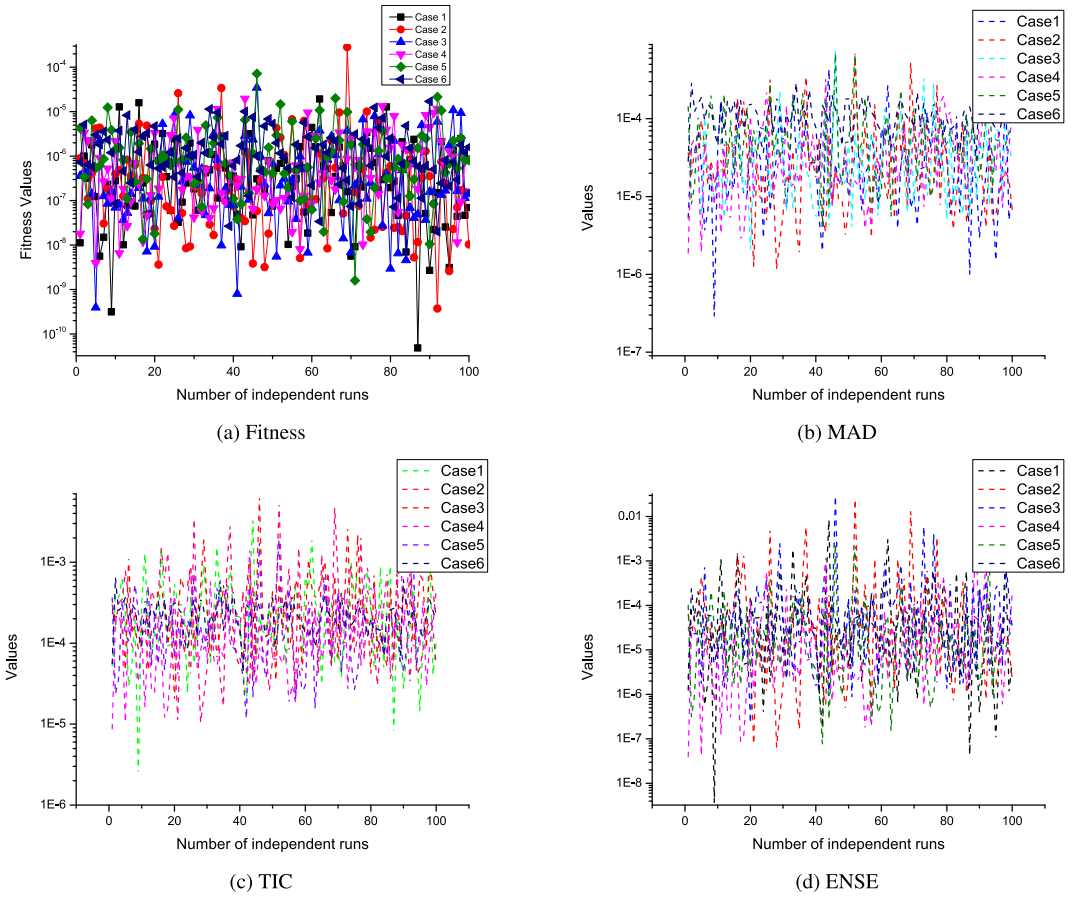

FIGURE 7. History plots for values of (a) fitness function (b) MAD (C) TIC (d) ENSE recorded during 100 simulations, obtained at the end of each experiment, for six cases of CSM.

of terms. Therefore, integer derivatives are ''local'' operators whereas fractional derivatives have, implicitly, a ''memory'' of all past events. However, the influence of past events decreases over time. The formulation in (13) inspires a discrete time calculation presented by the following definition.

Definition 2: The signal $D^{\alpha}[x[t]]$ given by [47]

$$D^{\alpha}[x[t]] = \frac{1}{T^{\alpha}} \sum_{k=0}^{r} \frac{(-1)^{k} \Gamma[\alpha+1] x[\text{t-k}T]}{\Gamma[k+1]\Gamma[\alpha-k+1]} \tag{14}$$

where T is the sampling period and r is the truncation order, is the approximate discrete time Grünwald–Letnikov fractional difference of order α, $\alpha \in C$, of the generic discrete signal $x(t)$. The series presented in equation (14) can be implemented by a rational fraction expansion that leads to a superior compromise in what concerns the number of terms versus the quality of the approximation.

C. SEARCH METHODOLOGY OF FO-DPSO

According to recent studies, fractional calculus (FC) attracted many researchers to apply it in defining and solving problems arising in engineering [47], applied mathematics, mechanical/ dynamics, [48], [49]. Grunwald-Letnikov defined fractional derivative containing fractional coefficients $\alpha \epsilon C$, a real number, by varying an unknown function $x(t)$ as in equation (15)

$$D^{\alpha}[x(t)] = \lim_{h \to 0} \left[\frac{1}{h^{\alpha}} \sum_{k=0}^{+\infty} \frac{(-1)^{k} \Gamma(\alpha+1) x(t-kh)}{\Gamma(k+1)\Gamma(\alpha-k+1)} \right] \tag{15}$$

where the symbol Γ represent gamma function. It is further elaborated that in equation (15), if the derivative is of integer order, then the series is defined by finite terms. On the other hand, if α is of fractional order the result is represented by the infinite term. Therefore, it is interesting to note that ordinary derivatives are local/instantaneous operators while fractional operators represent the memory of past changes. Moreover, the memory of past instances decreases with time. A derivative for discrete instances is defined in equation (16),

$$D^{\alpha}[x(t)] = \frac{1}{T^{\alpha}} \left[\sum_{k=0}^{r} \frac{(-1)^{k} \Gamma(\alpha+1) x(t-kh)}{\Gamma(k+1)\Gamma(\alpha-k+1)} \right] \tag{16}$$

The term T denotes time intervals of events occurred and truncated terms are represented by r. Tools existing in

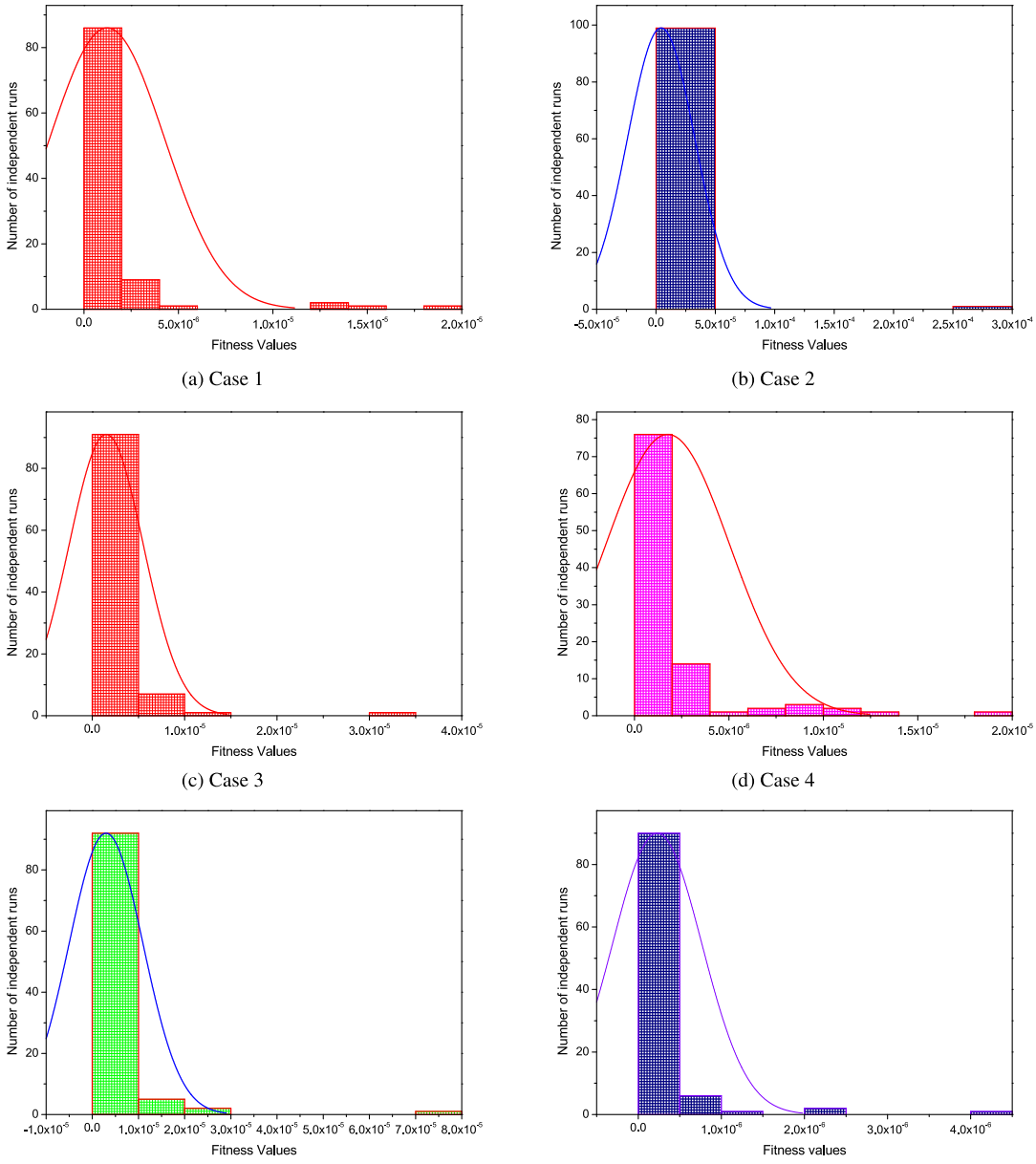

(a) Case 1 (b) Case 2

(c) Case 3 (d) Case 4

(e) Case 5 (f) Case 6

FIGURE 8. **Normal probability plots of fitness values obtained during 100 experiments for six cases.**

fractional calculus are useful in irreversible and chaotic processes, because of their memory keeping characteristics. Keeping in view the chaotic behavior of swarms in the Darwinian Particle swarms optimization algorithm, fractional calculus tools are suitable to keep track of past moves by swarms. Assuming the inertial weight in FO-DPSO $w = 1$, T as 1 and keeping in view the work done in [50], we get the following expression,

$$D^{\alpha}[v_{t+1}^{n}] = \rho_1 r_1(\breve{g}_t^n - x_t^n) + \rho_2 r_2(\breve{x}_t^n - x_t^n) + \rho_3 r_3(\breve{n}_t^n - x_t^n) \tag{17}$$

Empirical results produced by the algorithm are the same for $r \geq 4$. Also, the computational complexity increases linearly and thus occupy $O(r)$ memory. Hence for faster convergence, the fifth term and onwards are truncated. Thus the value of r is kept as 4. Adding these four terms of differential derivative the velocity term in FO-DPSO [45] becomes as in equation (18),

$$\begin{aligned} v_{t+1}^{n} = {} & \alpha v_t^n + \frac{1}{2}\alpha v_{t-1}^n + \frac{1}{6}\alpha(1-\alpha)v_{t-2}^n \\ & + \frac{1}{24}\alpha(1-\alpha)(2-\alpha)v_{t-3}^n \qquad (18) \\ & + \rho_1 r_1(\breve{g}_t^n - x_t^n) \\ & + \rho_2 r_2(\breve{x}_t^n - x_t^n) + \rho_3 r_3(\breve{n}_t^n - x_t^n) \qquad (19) \end{aligned}$$

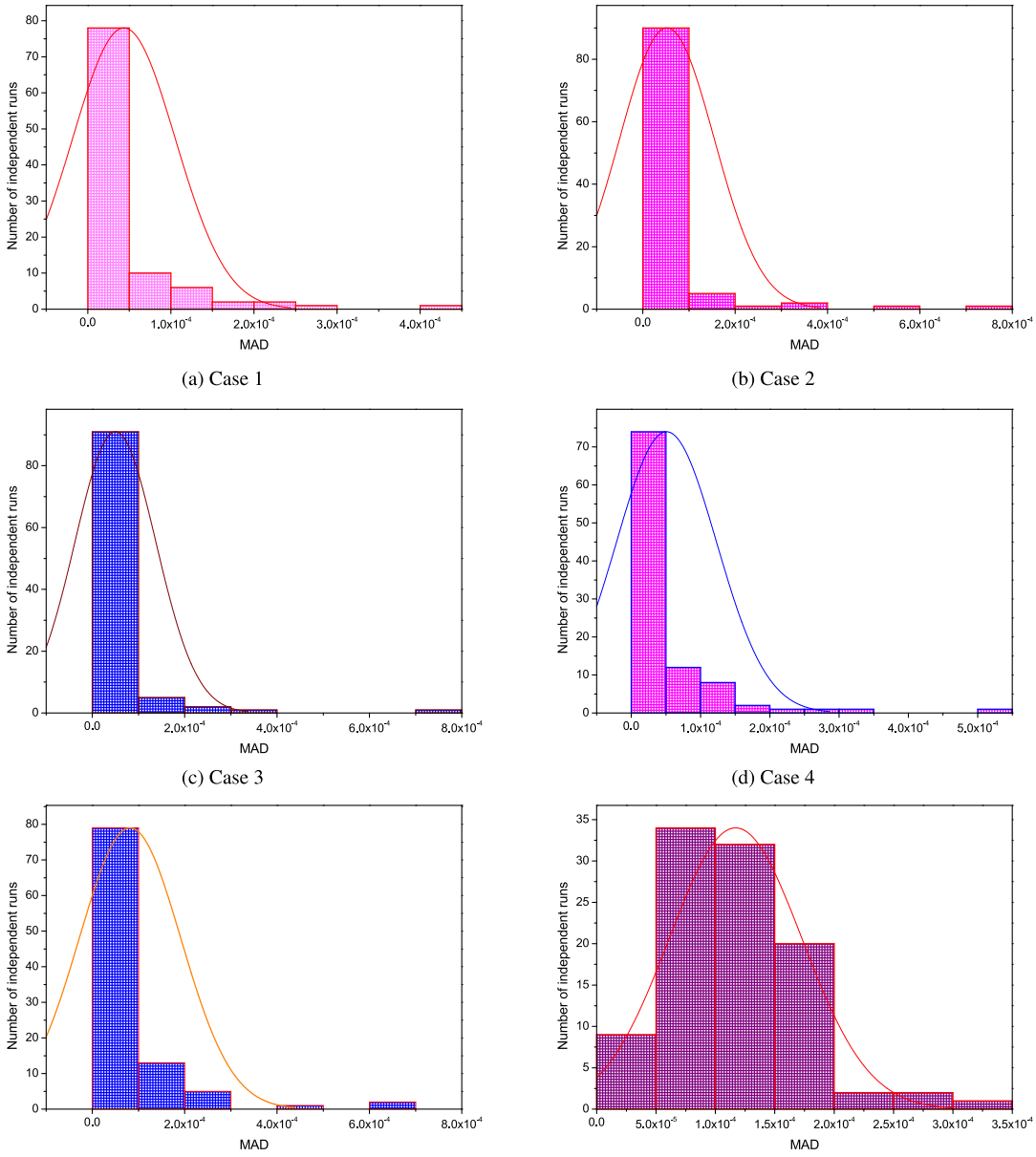

FIGURE 9. Normal probability plots of MAD values obtained during 100 experiments for six cases.

D. CONVERGENCE THEORY OF FO-DPSO

Experimental results show that the convergence of the algorithm depends upon the fractional order α. However, contrary to the FOPSO presented in [50], the Darwinian algorithm easily avoids being stuck in local solutions independently of the value of α (because it is a particularity of the traditional DPSO). Moreover, one can observe that, in most situations, a faster optimization convergence is obtained for a fractional coefficient α in the range [0.5, 0.8]. Therefore, to evaluate the FODPSO further, let us then systematically adjust the fractional coefficient a between 0.5 and 0.8, according to the expression:

$$\alpha(t) = 0.8 - 0.3\frac{t}{2000}. \tag{20}$$

III. STATISTICAL EVALUATION

In the present study, we give statistical analysis for all the cases of the CSM, which are based on mean, standard deviation, and minimum values. Performance matrices like MAD, TIC, and ENSE are used to test the efficiency of our approach in each simulation while global performance matrices like GMAD, GTIC, GFIT, and GENSE are used to test the global efficiency of our novel approach. We give the mathematical formulation for these performance matrices in equations (16-19)

$$\text{MAD} = \frac{1}{n}\sum_{m=1}^{n} |y(t_m) - \widehat{y}(t_m)| \tag{21}$$

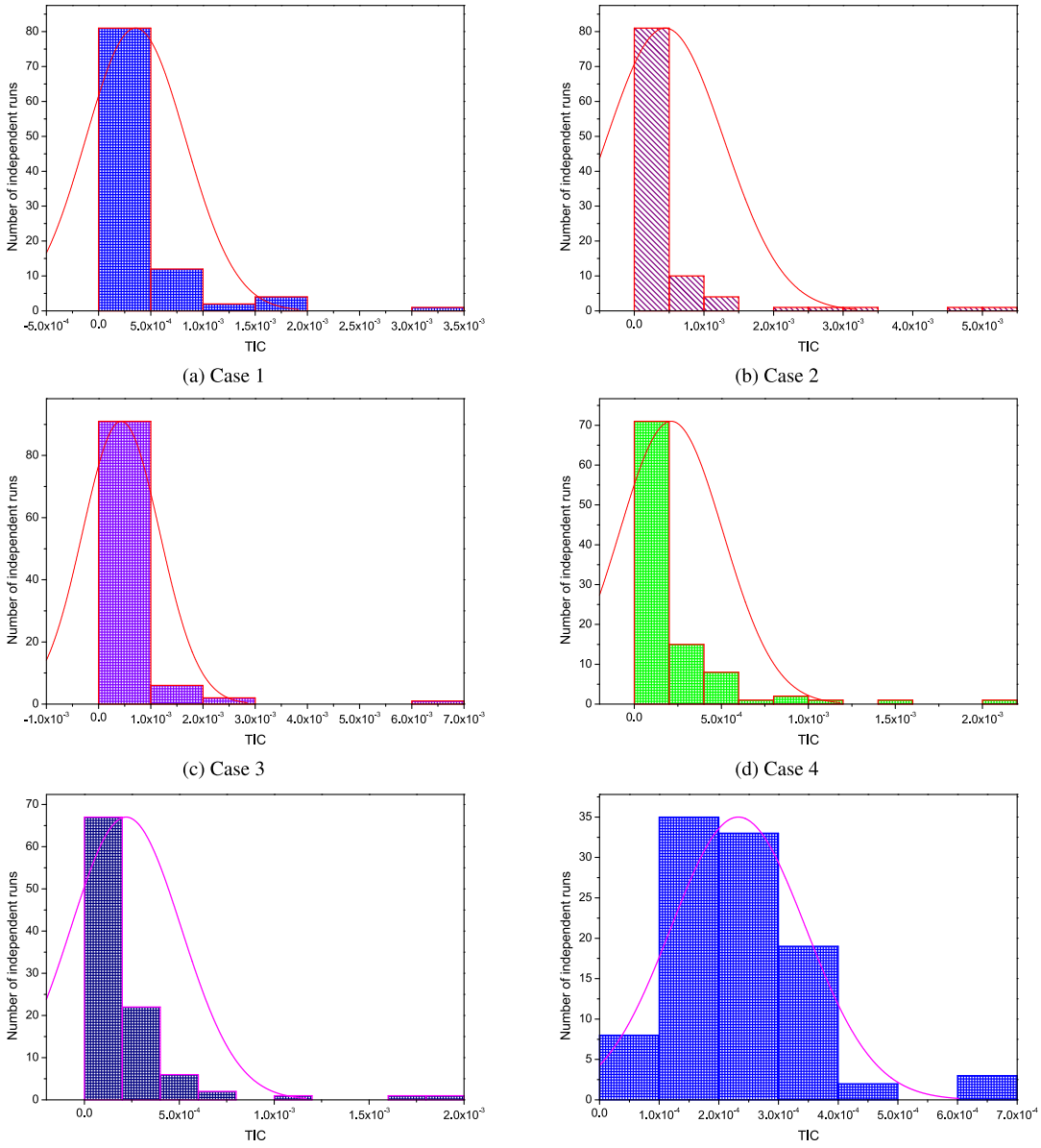

FIGURE 10. Normal probability plots of TIC values obtained during 100 experiments for six cases.

$$\mathrm{TIC} = \frac{\sqrt{\frac{1}{n}\sum_{m=1}^{n}\left(y(t_m)-\widehat{y}(t_m)\right)^2}}{\sqrt{\frac{1}{n}\sum_{m=1}^{n}(\widehat{y}(t_m))^2)}+\sqrt{\frac{1}{n}\sum_{m=1}^{n}(\widehat{y}(t_m))^2}} \tag{22}$$

$$\mathrm{NSE} = \left\{1-\frac{\sum_{m=1}^{n}\left(y(t_m)-\widehat{y}(t_m)\right)^2}{\sum_{m=1}^{n}\left(y(t_m)-\bar{y}(t_m)\right)^2}, \right. \tag{23}$$

$$\bar{y}(t_m) = \frac{1}{n}\sum_{m=1}^{n} y(t_m)$$

$$\mathrm{E_{NSE}} = 1-\mathrm{NSE} \tag{24}$$

$$GMAD = \frac{1}{R}\sum_{r=1}^{R}\left(\frac{1}{m}\sum_{i=1}^{m}\left(\left|h\left(t_i\right)-\hat{h}\left(t_i\right)\right|\right)\right) \tag{25}$$

$$GFIT = \frac{1}{R}\sum_{r=1}^{R} e_r \tag{26}$$

$$GENSE = \frac{1}{R}\sum_{r=1}^{R}\left(\sqrt{\frac{1}{m}\sum_{i=1}^{m}\left(h\left(t_i\right)-\hat{h}\left(t_i\right)\right)^2}\right) \tag{27}$$

In the case, if a perfect solution approaches then all the values of MAD, TIC and ENSE become zero.

IV. SIMULATIONS AND RESULTS

In this section, we considered six different cases for the CSM and performed 100 independent numerical simulations to see the robustness of our approach.

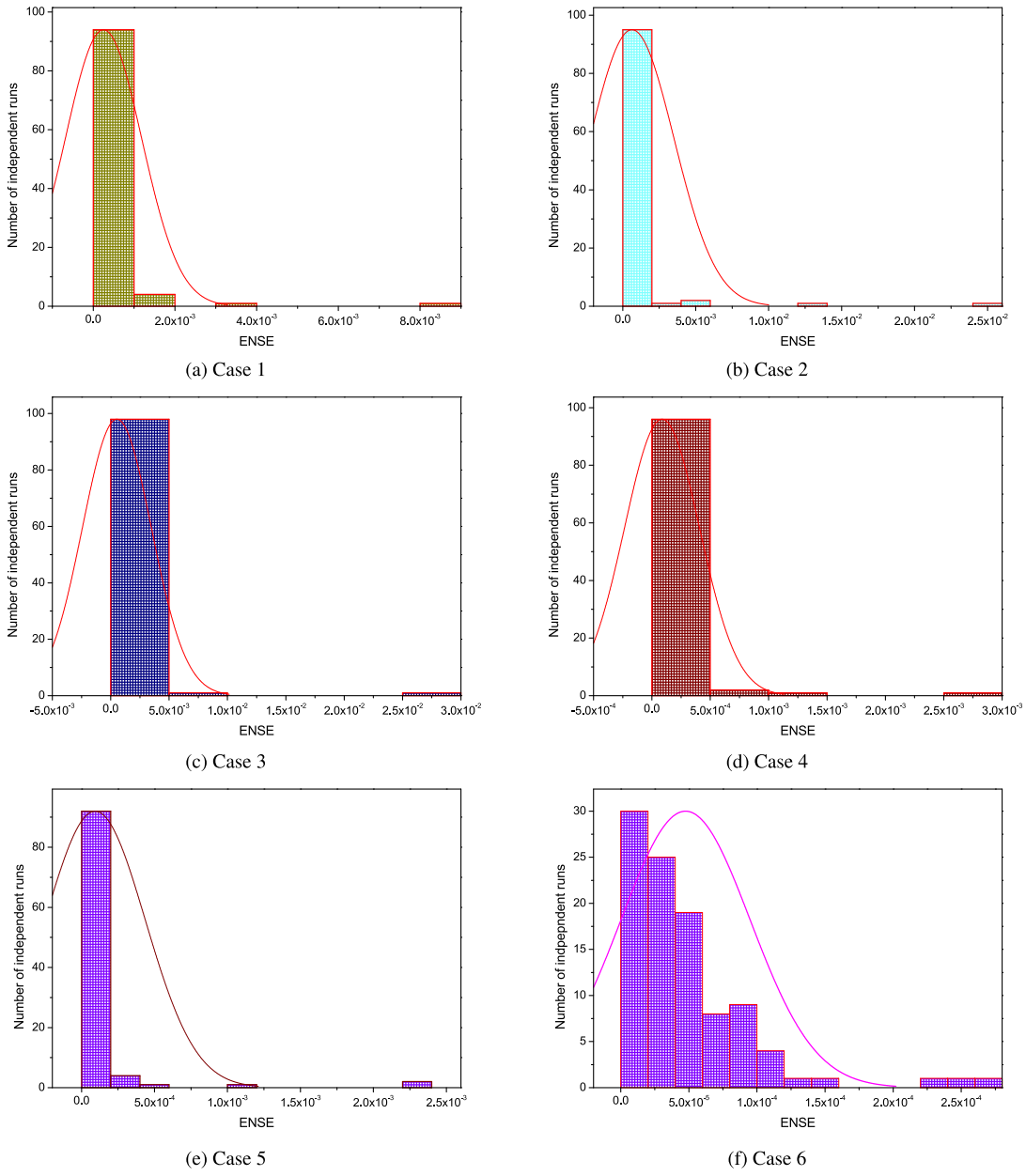

FIGURE 11. Normal probability plots of ENSE values obtained during 100 experiments for six cases.

A. CASE 1

By considering c=d=0.1 in equation (3), and choosing the interval $x \in [0, 1]$ becomes as:

$$\begin{cases} \chi'' - 0.1\chi + \dfrac{0.1}{\sqrt{1+\chi'^2}} = 0 \\ \chi'(0) = \chi(1) = 0 \text{ in } [0, 1] \end{cases} \tag{28}$$

The fitness evaluation of the case 1 is:

$$\zeta = \frac{1}{N}\sum_{k=1}^{N}(\sqrt{1+\chi'^2}\hat{\chi}_k'' - 0.1\sqrt{1+\chi'^2}\hat{\chi} + 0.1)^2 + \frac{1}{2}\left((\hat{\chi}_0')^2 + (\hat{\chi}_N)^2\right) \tag{29}$$

B. CASE 2

Taking the values of $c = 0.2$, $d = 0.1$ in CSM (3) using the interval $x \in [0, 1]$.

C. CASE 3

Taking the values of $c = 0.3$, $d = 0.1$ in CSM (3) using the interval $x \in [0, 1]$.

D. CASE 4

Taking the values of $c = 0.1$, $d = 0.2$ in CSM (3) using the interval $x \in [0, 1]$.

E. CASE 5

Taking the values of $c = 0.1$, $d = 0.3$ in CSM (3) using the interval $x \in [0, 1]$.

TABLE 1. AE obtained for case 1, 2 and 3 for CSM.

	Case1				Case2				Case3			
x	Min PSO-ASA	Min FO-DPSO	Mean	STD	Min PSO-ASA	Min FO-DPSO	Mean	STD	Min PSO-ASA	Min FO-DPSO	Mean	STD
0	1.02E-08	1.04E-11	1.96E-07	7.04E-07	3.49E-08	1.74E-11	3.28E-07	1.67E-06	7.87E-09	7.26E-11	1.61E-07	3.99E-07
0.1	1.70E-08	1.03E-11	1.43E-07	5.66E-07	3.05E-08	1.21E-10	6.91E-07	5.15E-06	1.56E-08	6.02E-11	7.48E-08	2.20E-07
0.2	4.64E-09	8.26E-12	9.38E-08	3.62E-07	1.18E-08	3.58E-12	2.13E-07	1.28E-06	2.74E-08	5.55E-11	8.61E-08	2.87E-07
0.3	2.80E-08	9.73E-14	4.85E-08	9.71E-08	2.00E-09	7.32E-11	3.51E-07	2.51E-06	2.18E-08	5.75E-12	9.39E-08	2.61E-07
0.4	3.45E-09	3.18E-12	9.66E-08	3.25E-07	1.23E-08	1.52E-11	3.21E-07	2.39E-06	1.31E-08	6.87E-13	6.08E-08	1.57E-07
0.5	7.17E-08	5.28E-12	6.91E-08	1.77E-07	5.16E-09	1.65E-11	2.16E-07	1.46E-06	2.56E-09	3.81E-13	7.00E-08	1.92E-07
0.6	2.15E-08	1.62E-12	7.20E-08	2.27E-07	2.37E-08	4.76E-11	4.27E-07	3.10E-06	7.26E-10	6.81E-13	1.04E-07	3.60E-07
0.7	3.92E-08	2.66E-13	8.91E-08	2.19E-07	3.86E-09	6.16E-12	3.17E-07	1.83E-06	5.64E-10	6.60E-14	1.32E-07	3.98E-07
0.8	8.97E-09	3.68E-12	7.60E-08	2.03E-07	9.84E-10	1.96E-11	3.25E-07	2.43E-06	2.85E-09	3.00E-11	1.14E-07	2.83E-07
0.9	1.89E-09	2.71E-12	4.08E-08	9.34E-08	3.70E-10	3.33E-11	6.48E-07	6.01E-06	1.84E-09	8.11E-11	5.58E-08	1.80E-07
1	1.20E-10	2.84E-12	2.98E-07	8.87E-07	4.72E-11	1.94E-11	4.76E-07	1.46E-06	7.52E-12	8.89E-11	5.40E-07	1.84E-06

TABLE 2. AE obtained for case 4, 5 and 6 for CSM.

	Case 4				Case 5				Case 6			
x	Min PSO-ASA	Min FO-DPSO	Mean	STD	Min PSO-ASA	Min FO-DPSO	Mean	STD	Min PSO-ASA	Min FO-DPSO	Mean	STD
0	5.63E-09	7.61E-10	1.97E-07	4.94E-07	4.76E-08	1.21E-10	2.82E-07	2.51E-06	1.19E-08	4.40E-10	2.28E-07	5.38E-07
0.1	7.11E-08	8.83E-10	1.36E-07	3.75E-07	1.17E-07	7.74E-11	6.33E-10	7.46E-07	8.50E-09	1.06E-09	2.50E-07	4.22E-07
0.2	1.11E-07	6.64E-10	1.15E-07	2.61E-07	2.72E-07	9.70E-11	3.70E-07	3.55E-07	5.45E-09	8.38E-11	1.67E-07	3.42E-07
0.3	1.04E-08	1.26E-12	1.05E-07	2.72E-07	3.43E-07	7.66E-13	1.14E-07	3.42E-07	1.47E-08	2.00E-09	1.04E-07	2.31E-07
0.4	2.91E-09	3.49E-10	1.04E-07	2.41E-07	2.40E-07	7.23E-11	9.18E-08	5.77E-07	4.45E-08	2.40E-09	1.59E-07	2.82E-07
0.5	1.76E-08	5.09E-10	1.01E-07	2.36E-07	1.78E-07	1.68E-10	2.89E-07	7.63E-07	2.74E-08	4.62E-10	1.63E-07	2.46E-07
0.6	1.78E-09	1.32E-10	7.34E-08	1.81E-07	1.99E-08	1.59E-10	1.99E-07	7.17E-07	3.15E-08	4.72E-10	9.20E-08	1.68E-07
0.7	6.68E-09	3.23E-11	1.39E-07	2.97E-07	4.13E-08	1.12E-10	3.85E-07	6.38E-07	2.60E-08	3.35E-09	1.40E-07	2.91E-07
0.8	3.36E-08	2.94E-10	2.29E-07	5.07E-07	8.95E-09	7.08E-11	3.01E-07	5.70E-07	1.98E-08	4.18E-09	3.05E-07	4.15E-07
0.9	3.24E-09	1.64E-10	7.27E-08	1.71E-07	2.41E-08	1.36E-12	4.89E-07	2.40E-07	1.27E-08	6.54E-10	1.63E-07	2.13E-07
1	1.46E-11	1.45E-10	4.78E-07	1.16E-06	1.64E-11	7.11E-10	4.45E-07	2.15E-06	3.09E-11	4.60E-09	4.82E-07	7.71E-07

TABLE 3. Results for global Fitness, MAD, TIC and ENSE for each case of the CSM.

	GFIT		GMAD		GTIC		GENSE	
Case	Mean	STD	Mean	STD	Mean	STD	Mean	STD
1	1.23E-06	3.05E-06	4.35E-05	6.18E-05	3.54E-04	1.23E-02	2.52E-04	9.35E-04
2	4.32E-06	2.84E-05	5.21E-05	1.02E-04	4.42E-04	8.46E-04	6.30E-04	2.90E-03
3	1.50E-06	4.03E-06	4.99E-05	6.10E-06	8.79E-05	7.41E-04	5.27E-04	3.00E-03
4	1.76E-06	3.29E-06	5.08E-05	7.23E-05	2.12E-04	2.98E-04	8.66E-05	3.22E-04
5	2.97E-06	8.01E-06	8.16E-05	1.10E-04	2.20E-04	2.92E-04	9.31E-05	3.44E-04
6	2.26E-06	2.96E-06	1.17E-04	5.59E-05	2.33E-04	1.13E-04	4.76E-05	4.74E-05

F. CASE 6

Taking the values of $c = 0.1$, $d = 0.4$ in CSM (3) using the interval $x \in [0, 1]$.

Best solutions for all cases are given in Fig 3. The unknown weights involved in calculation of best solutions are visualized in Fig. 4. Also Fig. 5 represents the set of residual errors for all six cases obtained for best solutions. The domain of the problem is the interval [0, 1] and by taking the step size 0.1. From Fig. 3 it is evident that our solutions and reference solutions are in agreement with each other for each point. To ensure the stability and effectiveness of our algorithm we have compared our results obtained from 100 simulations with the reference solutions to decide the best result for each case of CSM. Fig. 6 depicts the best, mean and worse values of fitness, MAD, TIC, and ENSE for all six cases. The values of absolute errors (AE) in tables 1 and 2 lie around 10^{-11} to 10^{-14}, 10^{-10} to 10^{-12}, 10^{-11} to 10^{-14}, 10^{-10} to 10^{-12}, 10^{-10} to 10^{-13} and 10^{-09} to 10^{-11} for best solutions. While it ranges from 10^{-07} to 10^{-08}, 10^{-06} to 10^{-07}, 10^{-07} to 10^{-08}, 10^{-07} to 10^{-08}, 10^{-07} to 10^{-08} and 10^{-06} to 10^{-08} for mean solutions. For worst solutions the AE lie around 10^{-01} to 10^{-03}, 10^{-01} to 10^{-03}, 10^{-03} to 10^{-04}, 10^{-02} to 10^{-03}, 10^{-04} to 10^{-05} and 10^{-04} to 10^{-05} for all the cases of CSM [41]. All the result proves very good agreements. In Fig. 7, we present history plots for values of the fitness function, MAD, TIC, ENSE recorded during 100 simulations, obtained at the end of each experiment, for six cases of CSM. It is clear in the table. 3 that mean values of GFIT are 1.23E-06, 4.32E-06, 1.50E-06, 1.76E-06, 2.97E-06, 2.26E-06 for cases 1 to 6 respectively. Mean values of GMAD are 4.35E-05, 5.21E-05, 4.99E-05, 5.08E-05, 8.16E-05, 1.17E-04 for cases 1 to 6 respectively. Mean values of GTIC are 3.54E-04, 4.42E-04, 8.79E-05, 2.12E-04, 2.20E-04, 2.33E-04 for

TABLE 4. Computational cost in terms of CPU time(s), iterations, and function evaluations for each problem of CSM.

Problem	Time PSO-ASA	Time FO-DPSO	Iteration PSO-ASA	Iteration FO-DPSO	Function evaluation PSO-ASA	Function evaluation FO-DPSO
1	56.1961002	28.843141	4241.96	2000	294677.84	200000
2	58.3110227	27.747841	4428.65	2000	308112.95	200000
3	48.6112643	26.621021	3724.91	2000	259830.29	200000
4	61.2390527	26.58257	4682.46	2000	325474.67	200000
5	78.3866805	27.543034	5227.86	2000	363201.65	200000
6	87.9105152	27.25125	5480.43	2000	380791.59	200000

TABLE 5. Maximum error obtained using different number of neurons.

x	N=10	N=8	N=5
0	1.04E-11	4.53E-10	1.03E-07
0.1	1.03E-11	9.71E-12	1.03E-08
0.2	8.26E-12	3.58E-09	6.70E-08
0.3	9.73E-14	1.73E-10	5.47E-08
0.4	3.18E-12	4.63E-09	1.11E-08
0.5	5.28E-12	8.47E-09	3.35E-09
0.6	1.62E-12	8.86E-10	3.84E-08
0.7	2.66E-13	6.11E-09	6.74E-08
0.8	3.68E-12	2.19E-08	4.40E-08
0.9	2.71E-12	7.10E-09	2.32E-10
1	2.84E-12	3.93E-08	1.21E-07

cases 1 to 6 respectively and mean values of GENSE are 2.52E-04, 6.30E-04, 5.27E-04, 8.66E-05, 9.31E-05, 4.76E-05 for cases 1 to 6 respectively. The computational cost of our procedure is measured in terms of CPU time, iterations, and function evaluations taken to solve all 6 problems see table 4. Our approach requires less time, minimum iterations and function evaluations to achieve results of the required standard as compared to results reported in [41]. All the inputs are continuous and as in Fig 3 with small changes in different terms involved in our mathematical model, the solution is stable and shows small variations. Thus our model under consideration is well-conditioned. All these global performance matrices indicate our soft computing design is much competitive as compared to the state-of-the-art techniques. Normal probability plots see Figs. 8-11 indicate that values of fitness, MAD, TIC, and ENSE are very small for 100 experiments considering six cases of CSM.

V. CONCLUSION

The research done in this paper is concluded by the following remarks,

1) We have designed a new soft computing procedure, by which we have calculated solutions for the corneal shape model. Feed-Forward ANNs are used to approximate the general solutions for the CSM model. The unknown weights involved in the general solutions are trained by a well balanced Nature-inspired technique which is named FO-DPSO. This optimization technique is proved to be a good global search as well as a local search technique. Fitness functions were defined based on the residual errors in approximate solutions which we have tried to minimize by using FO-DPSO.
2) To establish the good performance of the ANN-based FO-DPSO procedure, we have chosen Adams's numerical solver as a reference solution calculator. Different scenarios are considered for CSM. In all cases, ANN-based FO-DPSO was better in terms of getting more accurate solutions with less residual errors.
3) Statistical terms like mean, minimum, standard deviations are calculated for results obtained from 100 independent simulations with different initial populations. It was confirmed that our procedure is an important and suitable candidate for solving mathematical models representing real-world problems.
4) In all scenarios of CSM, our procedure was better in terms of less number of function evaluations, mean time value, ENSE, TIC, MAD. This procedure can be used for partial differential equations and fractional-order differential equations with some modifications.

In the future, we will implement this technique for different real-world problems with fractional derivatives to have a deep insight. More convergence analysis is required to explain the FO-DPASO base ANN procedure.

APPENDIX

$$\begin{aligned}\chi(x)_{case1} = {} & \frac{0.695831459561791}{1+e^{-(-0.445461691716731x+0.559464015362682)}} \\ & + \frac{0.857202437729070}{1+e^{-(-0.237526067375416t-3.95847296398435)}} \\ & + \frac{-3.21486042159391}{1+e^{-(-0.870159531592183x-3.65902542008718)}} \\ & + \frac{0.734665852064563}{1+e^{(-0.517619339223332x+1.97547424788769)}} \\ & + \frac{-0.0102791099323604}{1+e^{-(-0.429818013212879x+0.0384072956774085)}} \\ & + \frac{-0.194780517438811}{1+e^{-(0.798300190831507x+4.99089976751116)}} \\ & + \frac{0.642716229430733}{1+e^{-(-1.48666033825261x-4.34661230033876)}} \\ & + \frac{0.00176645580297596}{1+e^{-(1.84308030858239x-0.780906274299805)}} \\ & + \frac{-1.90296667674946}{1+e^{-(-0.223817599065422x-0.482445193295733)}} \\ & + \frac{-1.87685224934406}{1+e^{-(0.726112779383839x-3.42642740470645)}} \end{aligned} \tag{30}$$

$$\begin{aligned}\chi(x)_{case2} = {} & \frac{-0.274974243710526}{1+e^{-(0.585914908005785x+2.01062679578643)}} \\ & + \frac{0.0708536574547530}{1+e^{-(1.79328228238756x-0.211844967936489)}}\end{aligned}$$

$$+\frac{0.842629748467294}{1+e^{-(1.74525992098521x+5)}}+\frac{-0.116399036336741}{1+e^{-(-2.24263701983815x-1.88296059313356)}}+\frac{0.384028095593582}{1+e^{-(0.872088417762822x+0.929854833335827)}}+\frac{-1.18255492549412}{1+e^{-(0.269169438317497x+5)}}+\frac{1.09529790391014}{1+e^{-(-0.511879060722408x+1.79064742640828)}}+\frac{0.0903768171622611}{1+e^{-(1.46719482455247x-1.87200278559390)}}+\frac{-1.20152474138597}{1+e^{-(0.774340068680691x-3.36644142561565)}}+\frac{-0.644304866967837}{1+e^{-(0.602622179846140x+2.13305430308015)}} \quad (31)$$

$$\chi(x)_{case3}=\frac{1.14524767300943}{1+e^{-(0.497085905477655x+1.03150626269979)}}+\frac{-3.09424545649312}{1+e^{-(0.625183502313801x-0.424807166590887)}}+\frac{-0.284406015833670}{1+e^{-(1.93368666265249x-4.48686677142058)}}+\frac{2.54653457465888}{1+e^{-(0.365930532381210x-0.244781460377318)}}+\frac{-2.19028605511111}{1+e^{-(-0.155198554043503x-2.86809120202160)}}+\frac{-0.834562572163173}{1+e^{-(-0.253520378861498x+3.39441634201052)}}+\frac{0.450238261169759}{1+e^{-(1.33867709748867x+2.92085528357334)}}+\frac{0.327267338363910}{1+e^{-(-1.41662034354300x-2.66993782102434)}}+\frac{-0.390319950295860}{1+e^{-(-1.03169182616878x+0.181013148152516)}}+\frac{-0.238081026579067}{1+e^{-(-1.88662657799308x-4.76981220991832)}} \quad (32)$$

$$\chi(x)_{case4}=\frac{-0.101394819777945}{1+e^{-(-0.324135662176636x+0.393000384067753)}}+\frac{-0.246237133474045}{1+e^{-(1.44918683346222x-2.78739450451830)}}+\frac{0.303842256080317}{1+e^{-(1.35102209843720x-0.0165031439973391)}}+\frac{0.570447571542129}{1+e^{-(-1.82308843106756x-3.73701466970324)}}+\frac{-2.27559047367201}{1+e^{-(1.14835598489040x-4.33439259443281)}}+\frac{-0.419770900949776}{1+e^{-(-0.959775771651920x-3.57961995185080)}}+\frac{-2.01123549346417}{1+e^{-(-0.817969935253694x-3.36674549112899)}}+\frac{-4.90538524897789}{1+e^{-(-1.22264924456206x-4.22228174943473)}}+\frac{0.584303013011058}{1+e^{-(-0.743591809789781x-0.0815087248865332)}}+\frac{-0.249187667299933}{1+e^{-(1.27098079114687x-0.486572443190713)}} \quad (33)$$

$$\chi(x)_{case5}=\frac{-1.65328360998710}{1+e^{-(0.794356626908655x-1.50745356670287)}}+\frac{0.303728749117813}{1+e^{-(-1.44893547538213x+0.442396978992330)}}+\frac{0.0967770715437123}{1+e^{-(-1.91240500519205x-0.744850660599771)}}+\frac{0.598011681888485}{1+e^{-(-0.246770044909789x-1.66592597570062)}}+\frac{0.0278344629630608}{1+e^{-(0.703194533215742x+0.0450969442192352)}}+\frac{-1.23844017594612}{1+e^{-(0.847420428907692x-3.63939018570850)}}+\frac{0.867239186998636}{1+e^{-(-0.101056136698669x+2.80195342805364)}}+\frac{-1.50615470819223}{1+e^{-(-1.00799846322235x-0.359652017118539)}}+\frac{-0.818121427741594}{1+e^{-(-1.63451487995171x-3.34235608433912)}}+\frac{-0.981672246350874}{1+e^{-(1.22661880304038x-3.80134572115877)}} \quad (34)$$

$$\chi(x)_{case6}=\frac{-2.24689821707894}{1+e^{-(0.673951497675586x+0.165082329242494)}}+\frac{-0.126706702662168}{1+e^{-(0.650298520767727x+2.12846296339058)}}+\frac{1.06039609262931}{1+e^{-(-1.78809137415529x+4.99998744679029)}}+\frac{-1.71914357460005}{1+e^{-(-0.970162952685123x-0.114127356658791)}}+\frac{0.358351015787281}{1+e^{-(-1.34392603786262x-0.593102390652443)}}+\frac{1.72910571225798}{1+e^{-(-0.990302197825875x+1.76004772927106)}}+\frac{-2.21331926323089}{1+e^{-(-0.0372728879004384x+0.867050874857976)}}+\frac{0.154402171327691}{1+e^{-(1.22826775877717x+1.58383116761127)}}+\frac{-3.65559294557584}{1+e^{-(-0.633730448276276x-3.90016324810849)}}+\frac{1.36826099946251}{1+e^{-(1.31281713461553x+1.81279094808111)}} \quad (35)$$

REFERENCES

[1] I. Coelho, C. Corsato, and P. Omari, "A one-dimensional prescribed curvature equation modeling the corneal shape," *Boundary Value Problems*, vol. 2014, no. 1, p. 127, 2014.

[2] G. S. L. Peh, R. W. Beuerman, A. Colman, D. T. Tan, and J. S. Mehta, "Human corneal endothelial cell expansion for corneal endothelium transplantation: An overview," *Transplantation*, vol. 91, no. 8, pp. 811–819, Apr. 2011.

[3] T. Almubrad and S. Akhtar, "Structure of corneal layers, collagen fibrils, and proteoglycans of tree shrew cornea," *Mol. Vis.*, vol. 17, p. 2283, Aug. 2011.

[4] Y. Komai and T. Ushiki, "The three-dimensional organization of collagen fibrils in the human cornea and sclera," *Investigative Ophthalmol. Vis. Sci.*, vol. 32, no. 8, pp. 2244–2258, 1991.

[5] J. A. West-Mays and D. J. Dwivedi, "The keratocyte: Corneal stromal cell with variable repair phenotypes," *Int. J. Biochem. Cell Biol.*, vol. 38, no. 10, pp. 1625–1631, Jan. 2006.

[6] E. C. Carlson, C.-Y. Liu, T.-I. Chikama, Y. Hayashi, C. W.-C. Kao, D. E. Birk, J. L. Funderburgh, J. V. Jester, and W. W.-Y. Kao, "Keratocan, a cornea-specific keratan sulfate proteoglycan, is regulated by Lumican," *J. Biol. Chem.*, vol. 280, no. 27, pp. 25541–25547, Jul. 2005.

[7] J. A. Rada, P. K. Cornuet, and J. R. Hassell, "Regulation of corneal collagen fibrillogenesis in vitro by corneal proteoglycan (Lumican and Decorin) core proteins," *Experim. Eye Res.*, vol. 56, no. 6, pp. 635–648, Jun. 1993.

[8] S. Akhtar, A. J. Bron, A. J. Hayes, K. M. Meek, and B. Caterson, "Role of keratan sulphate (sulphated poly -N-acetyllactosamine repeats) in keratoconic cornea, histochemical, and ultrastructural analysis," *Graefe's Arch. Clin. Experim. Ophthalmol.*, vol. 249, no. 3, pp. 413–420, Mar. 2011.

[9] W. W.-Y. Kao and C.-Y. Liu, "Roles of lumican and keratocan on corneal transparency," *Glycoconjugate J.*, vol. 19, no. 4/5, pp. 275–285, May 2002.

[10] C. L. Chen and Y. C. Liu, "Solution of two-point boundary-value problems using the differential transformation method," *J. Optim. Theory Appl.*, vol. 99, no. 1, pp. 23–35, Oct. 1998.

[11] B. Jang, "Two-point boundary value problems by the extended Adomian decomposition method," *J. Comput. Appl. Math.*, vol. 219, no. 1, pp. 253–262, 2008.

[12] J. Lu, "Variational iteration method for solving two-point boundary value problems," *J. Comput. Appl. Math.*, vol. 207, no. 1, pp. 92–95, Oct. 2007.

[13] M. Abukhaled, S. Khuri, and A. Sayfy, "A numerical approach for solving a class of singular boundary value problems arising in physiology," *Int. J. Numer. Anal. Model.*, vol. 8, no. 2, pp. 353–363, 2011.

[14] P. Malekzadeh, M. R. Golbahar Haghighi, and M. M. Atashi, "Free vibration analysis of elastically supported functionally graded annular plates subjected to thermal environment," *Meccanica*, vol. 46, no. 5, pp. 893–913, Oct. 2011.

[15] F. M. Andrade, "Exact Green's function for rectangular potentials and its application to quasi-bound states," *Phys. Lett. A*, vol. 378, no. 21, pp. 1461–1468, Apr. 2014.

[16] S. Ahyoune, J. Sieiro, T. Carrasco, N. Vidal, J. M. López-Villegas, E. Roca, and F. V. Fernández, "Quasi-static PEEC planar solver using a weighted combination of 2D and 3D analytical Green's functions and a predictive meshing generator," *Integration*, vol. 63, pp. 332–341, Sep. 2018.

[17] M. M. M. Abukhaled, "Green's function iterative method for solving a class of boundary value problems arising in heat transfer," *Appl. Math. Inf. Sci.*, vol. 11, no. 1, pp. 229–234, Jan. 2017.

[18] M. Abukhaled and S. A. Khuri, "A semi-analytical solution of amperometric enzymatic reactions based on Green's functions and fixed point iterative schemes," *J. Electroanal. Chem.*, vol. 792, pp. 66–71, May 2017.

[19] H. Q. Kafri and S. A. Khuri, "Bratu's problem: A novel approach using fixed-point iterations and Green's functions," *Comput. Phys. Commun.*, vol. 198, pp. 97–104, Jan. 2016.

[20] M. A. Z. Raja, M. Umar, Z. Sabir, J. A. Khan, and D. Baleanu, "A new stochastic computing paradigm for the dynamics of nonlinear singular heat conduction model of the human head," *Eur. Phys. J. Plus*, vol. 133, no. 9, p. 364, Sep. 2018.

[21] L. Pastur-Romay, F. Cedrón, A. Pazos, and A. Porto-Pazos, "Deep artificial neural networks and neuromorphic chips for big data analysis: Pharmaceutical and bioinformatics applications," *Int. J. Mol. Sci.*, vol. 17, no. 8, p. 1313, 2016.

[22] D. Cangelosi, S. Pelassa, M. Morini, M. Conte, M. C. Bosco, A. Eva, A. R. Sementa, and L. Varesio, "Artificial neural network classifier predicts neuroblastoma patients' outcome," *BMC Bioinf.*, vol. 17, no. S12, p. 347, Oct. 2016.

[23] J. A. Khan, M. A. Z. Raja, M. M. Rashidi, M. I. Syam, and A. M. Wazwaz, "Nature-inspired computing approach for solving nonlinear singular Emden–fowler problem arising in electromagnetic theory," *Connection Sci.*, vol. 27, no. 4, pp. 377–396, Oct. 2015.

[24] M. A. Z. Raja, A. Mehmood, S. A. Niazi, and S. M. Shah, "Computational intelligence methodology for the analysis of RC circuit modelled with nonlinear differential order system," *Neural Comput. Appl.*, vol. 30, no. 6, pp. 1905–1924, Sep. 2018.

[25] M. A. Z. Raja, "Solution of the one-dimensional Bratu equation arising in the fuel ignition model using ANN optimised with PSO and SQP," *Connection Sci.*, vol. 26, no. 3, pp. 195–214, Jul. 2014.

[26] Z. Sabir, M. A. Manzar, M. A. Z. Raja, M. Sheraz, and A. M. Wazwaz, "Neuro-heuristics for nonlinear singular thomas-Fermi systems," *Appl. Soft Comput.*, vol. 65, pp. 152–169, Apr. 2018.

[27] I. Ahmad, F. Ahmad, M. A. Z. Raja, H. Ilyas, N. Anwar, and Z. Azad, "Intelligent computing to solve fifth-order boundary value problem arising in induction motor models," *Neural Comput. Appl.*, vol. 29, no. 7, pp. 449–466, Apr. 2018.

[28] M. A. Z. Raja, M. A. R. Khan, T. Mahmood, U. Farooq, and N. I. Chaudhary, "Design of bio-inspired computing technique for nanofluidics based on nonlinear Jeffery–Hamel flow equations," *Can. J. Phys.*, vol. 94, no. 5, pp. 474–489, May 2016.

[29] G. A. Silva, "A new frontier: The convergence of nanotechnology, brain machine interfaces, and artificial intelligence," *Frontiers Neurosci.*, vol. 12, p. 843, Nov. 2018.

[30] M. Umar, Z. Sabir, and M. A. Z. Raja, "Intelligent computing for numerical treatment of nonlinear prey–predator models," *Appl. Soft Comput.*, vol. 80, pp. 506–524, Jul. 2019.

[31] M. A. Z. Raja, "Stochastic numerical treatment for solving Troesch's problem," *Inf. Sci.*, vol. 279, pp. 860–873, Sep. 2014.

[32] M. A. Z. Raja, Z. Sabir, N. Mehmood, E. S. Al-Aidarous, and J. A. Khan, "Design of stochastic solvers based on genetic algorithms for solving nonlinear equations," *Neural Comput. Appl.*, vol. 26, no. 1, pp. 1–23, Jan. 2015.

[33] J. Motyl, "Upper separated multifunctions in deterministic and stochastic optimal control," *Appl. Math. Nonlinear Sci.*, vol. 2, no. 2, pp. 479–484, Nov. 2017.

[34] A. L. Edelen, S. G. Biedron, B. E. Chase, D. Edstrom, S. V. Milton, and P. Stabile, "Neural networks for modeling and control of particle accelerators," *IEEE Trans. Nucl. Sci.*, vol. 63, no. 2, pp. 878–897, Apr. 2016.

[35] A. K. Azad, L. Wang, N. Guo, H.-Y. Tam, and C. Lu, "Signal processing using artificial neural network for BOTDA sensor system," *Opt. Express*, vol. 24, no. 6, p. 6769, Mar. 2016.

[36] M. Pakdaman, A. Ahmadian, S. Effati, S. Salahshour, and D. Baleanu, "Solving differential equations of fractional order using an optimization technique based on training artificial neural network," *Appl. Math. Comput.*, vol. 293, pp. 81–95, Jan. 2017.

[37] J. Wang and J. Wang, "Forecasting stock market indexes using principle component analysis and stochastic time effective neural networks," *Neurocomputing*, vol. 156, pp. 68–78, May 2015.

[38] M. A. Z. Raja, A. K. Kiani, A. Shehzad, and A. Zameer, "Memetic computing through bio-inspired heuristics integration with sequential quadratic programming for nonlinear systems arising in different physical models," *SpringerPlus*, vol. 5, no. 1, p. 2063, Dec. 2016.

[39] M. A. Z. Raja, J. A. Khan, S. M. Shah, R. Samar, and D. Behloul, "Comparison of three unsupervised neural network models for first Painlevé transcendent," *Neural Comput. Appl.*, vol. 26, no. 5, pp. 1055–1071, Jul. 2015.

[40] W. Waseem, M. Sulaiman, S. Islam, P. Kumam, R. Nawaz, M. A. Z. Raja, M. Farooq, and M. Shoaib, "A study of changes in temperature profile of porous fin model using cuckoo search algorithm," *Alexandria Eng. J.*, vol. 59, no. 1, pp. 11–24, Feb. 2020.

[41] M. Umar, F. Amin, H. A. Wahab, and D. Baleanu, "Unsupervised constrained neural network modeling of boundary value corneal model for eye surgery," *Appl. Soft Comput.*, vol. 85, Dec. 2019, Art. no. 105826.

[42] G. Carleo and M. Troyer, "Solving the quantum many-body problem with artificial neural networks," *Science*, vol. 355, no. 6325, pp. 602–606, Feb. 2017.

[43] M. Hemmat Esfe, M. R. Hassani Ahangar, M. Rejvani, D. Toghraie, and M. H. Hajmohammad, "Designing an artificial neural network to predict dynamic viscosity of aqueous nanofluid of TiO2 using experimental data," *Int. Commun. Heat Mass Transf.*, vol. 75, pp. 192–196, Jul. 2016.

[44] S. Aidara, "Anticipated backward doubly stochastic differential equations with non-liphschitz coefficients," *Appl. Math. Nonlinear Sci.*, vol. 4, no. 1, pp. 101–112, Jun. 2019.

[45] M. S. Couceiro, R. P. Rocha, N. M. F. Ferreira, and J. A. T. Machado, "Introducing the fractional-order darwinian PSO," *Signal, Image Video Process.*, vol. 6, no. 3, pp. 343–350, Sep. 2012.

[46] J. A. Sabatier, S. Agrawal, and J. A. T. Machado, *Advances in Fractional Calculus*,vol. 4. Dordrecht, The Netherlands: Springer, 2007.

[47] J. T. Machado, M. F. Silva, R. S. Barbosa, I. S. Jesus, C. M. Reis, G. M. Marcos, and F. A. Galhano, "Some applications of fractional calculus in engineering," *Math. Problems Eng.*, vol. 2010, Nov. 2010, Art. no. 639801.
[48] I. Podlubny, "Fractional differential equations," in *Mathematics in Science and Engineering*, vol. 198. Melville, NY, USA: American Institute of Physics, 1999.
[49] R. F. Camargo, A. O. Chiacchio, and E. C. de Oliveira, "Differentiation to fractional orders and the fractional telegraph equation," *J. Math. Phys.*, vol. 49, no. 3, Mar. 2008, Art. no. 033505.
[50] E. J. S. Pires, J. A. T. Machado, P. B. de Moura Oliveira, J. Boaventura Cunha, and L. Mendes, "Particle swarm optimization with fractional-order velocity," *Nonlinear Dyn.*, vol. 61, nos. 1–2, pp. 295–301, Jul. 2010.

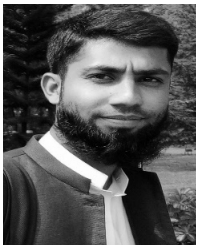

W. WASEEM received the B.S. degree in mathematics from Abdul Wali Khan University Mardan, in 2015, where he is currently pursuing the Ph.D. degree in mathematics. His research interests include optimization algorithms, real world problems, smart grids, and communications technology, and energy management.

MUHAMMAD SULAIMAN received the B.Sc., M.Sc., and M.Phil., degrees in mathematics from the University of Peshawar, and Quaid-e-Azam University, Islamabad, Pakistan, in 2004, 2007, and 2009, respectively, and the Ph.D. degree in mathematics from the University of Essex, U.K., in 2015.

From 2009 to 2016, he was a Lecturer of mathematics with the Abdul Wali Khan University Mardan, Pakistan. Since February 2016, he has been an Assistant Professor with the Department of Mathematics, Abdul Wali Khan University Mardan. He is the author of two book chapters, more than 15 articles. His research interests include optimization, including mathematical optimization techniques, global optimization, and evolutionary algorithms, heuristics, metaheuristics, multiobjective optimization, design engineering optimization problems, structural engineering optimization problems, linear programming, linear and non-linear least squares optimization problems, evolutionary algorithms, and nature-inspired metaheuristics. He is currently an Associate Editor of the journal COJ Reviews and Research, and the *SCIREA Journal of Mathematics*.

AHMAD ALHINDI (Member, IEEE) received the B.Sc. degree in computer science from Umm Al-Qura University (UQU), Makkah, Saudi Arabia, in 2006, and the M.Sc. degree in computer science and the Ph.D. degree in computing and electronic systems from the University of Essex, Colchester, U.K., in 2010 and 2015, respectively. He is currently an Assistant Professor of artificial intelligence (AI) with the Computer Science Department and a researcher in CIADA, UQU. His current research interests include evolutionary multiobjective optimization and machine learning techniques. He is involved in AI algorithms, focusing particularly on machine learning and optimization with a willingness to implement them in a context of decision making and solving combinatorial problems in real-world projects.

HOSAM ALHAKAMI received the B.Sc. degree in computer science from King Abdulaziz University, Saudi Arabia, in 2004, the M.Sc. degree in internet software systems from Birmingham University, Birmingham, U.K., in 2009, and the Ph.D. degree in software engineering from De Montfort University, in 2015. From 2004 to 2007, he worked in Software Development Industry, where he implemented several systems and solutions for a National Academic Institution. His research interests include algorithms, semantic web and optimization techniques. He focuses on enhancing real-world matching systems using machine learning and data analytics in a context of supporting decision-making.